Impact of Rain Heights on Rain-Induced Attenuation for Communication Systems Operating at Ka and V Bands in Pretoria, South Africa

Yusuf Babatunde Lawal
Department of Computer Systems Engineering
Tshwane University of Technology
Soshanguve South, South Africa
lawalyb@tut.ac.za

Pius A. Owolawi
Department of Computer Systems Engineering
Tshwane University of Technology
Soshanguve South, South Africa
owolawipa@tut.ac.za

Chunling Tu
Department of Computer Systems Engineering
Tshwane University of Technology
Soshanguve South, South Africa
duc@tut.ac.za

Etienne A. van Wyk
Department of Computer Systems Engineering
Tshwane University of Technology
Soshanguve South, South Africa
vanwykea@tut.ac.za

Joseph Sunday Ojo
Department of Physics
Federal University of Technology, Akure, Nigeria
ojojs_74@futa.edu.ng

2025 IEEE 15th Annual Computing and Communication Workshop and Conference (CCWC) | 979-8-3315-0769-5/25/$31.00 ©2025 IEEE | DOI: 10.1109/CCWC62904.2025.10903935

Abstract*— Wireless communication networks, such as 5G networks, inter-terrestrial, and earth-space links, transmit radio signals at high-frequency bands. However, the signal quality of radio communication systems operating at frequencies above 10 GHz in tropical and subtropical regions is often degraded due to rain-induced attenuation. Rain rate and rain height are the most influential meteorological parameters determining the level of attenuation. This research investigates the effects of seasonal variations in rain height on rain-induced attenuation and its impact on radio links operating at typical downlink and uplink frequencies in the Ka (30/20 GHz) and V (40/50 GHz) bands in Pretoria, South Africa. The research revealed that maximum rain heights experienced in the summer resulted in the worst rain-induced attenuation at all frequencies. The estimated attenuations would assist to determining the minimum fade margins required to achieve 99.9%, 99.99% and 99.999% signal availability annually at these frequencies in the study location. The results are expected to serve as a database for future planning of high-frequency link budgets.

***Keywords*—5G wireless networks, Earth-space link, Ka band, V band, Rain height, Rain-induced attenuation, Fade margin**

I. INTRODUCTION

The continuous demand for seamless superfast communication services can only be achieved by transmitting radio signals at high frequency. This is because transmission at high frequencies incorporates several advantages, such as high bandwidth, high data transfer rate, reduced antenna size, enhanced spatial resolution, etc. [1]-[4]. However, rain and oxygen gas are the major atmospheric components that poses severe threats to radio communication systems at high frequency. Attenuation due to rainwater droplet is of great concern in the scattering and absorption and subtropics due to frequent heavy rainfalls. Rain droplets degrade radio signals by scattering and absorption, which results in signal fading or total outage in severe conditions. The level of rain-induced attenuation experienced by a signal depends on factors such as transmission frequency, ground station height, elevation angle, effective path length, rain rate, rain height etc. These parameters can be varied to any desired values during link budget calculation except rain rate and rain height which are natural phenomena. Rain rate or rain intensity is a measure of the rainfall amount in a period of time on an area, while rain height is the altitude in the atmosphere at which precipitation starts forming in liquid water. Rain rate and rain height vary spatially and temporally due to seasonal variation of the local weather. Hence, the need for continuous studies to understand the seasonal variability and improve the estimation accuracy.

A rain rate of 1 minute integration time is required to deduce rain-induced attenuation. Several research studies have been conducted to measure it locally or convert available rain rates of higher integration time to 1minute rain rate. For instance, a study conducted in Beijing by Han *et al.* [5] analyzed rain-induced attenuation at 25 GHz and 38 GHz using local raindrop size distribution (DSD) of one minute integration. The research utilized empirically derived power-law coefficients to estimate specific attenuation which performed more accurately than the coefficients provided in the ITU-R model, highlighting the importance of localized data for precise attenuation prediction. An innovative approach known as the Quasi-Moment-Method (QMM) was recently proposed by Adekola *et al.* [6] to improve rain attenuation prediction. The proposed QMM algorithm provides computational advantages, and confirms better performance than previous models; thus, symbolizing potential for a number of improvements in further studies. The mass adoption of this method would require validation with directly measured rain attenuation in various regions. On the contrary, research on rainfall height statistics has received little attention due to the scarcity of ground-based rain radar in the research

location. In Satellite communication, rain height impacts slant path length, thereby affecting fade margin especially during wet season [7]. Seasonal variation of rain height remains a major consideration in the design of reliable inter-terrestrial microwave links and urban networks such as 5G mobile network. Accurate seasonal variation rain height data be used to optimized relay placement to mitigate the effects of rain attenuation.

The International Telecommunication Union (ITU) provided ITU-R P.837-7 and ITU-R P.839-4 databases, which recommend rain rates and rain heights for various regions, respectively [8]-[9]. Unfortunately, previous studies conducted in some regions have shown that the recommended values vary significantly from locally measured or derived values. A few of the previous studies discrepancies are reported below.

Lin *et al.* [10] emphasized the importance of seasonal rain height in calculating rain-induced attenuation, as the ITU-R annual mean rain height failed to predict attenuation accurately during heavy rainfall in China. Mandeep [11] applied radiosonde data to study the seasonal variation of rain height over Kuala Lumpur in Malaysia. The results confirmed that rain heights vary seasonally with peak values occurring in the months of May and October annually. The computed rain heights vary between 4.90 km and 5.20 km, while the fixed value prescribed by ITU-R P.839-4 is 4.94 km [11]. Similar research was conducted by Semire *et al.* [12] to cover eight locations in Malaysia. Studies conducted by Lawal *et al.* [13] and Lawal *et al.* [14] also confirmed the temporal and spatial variation of rain height over the four geoclimatic zones in Nigeria. The research reported varying rain heights between 5.08 km and 5.29 m, while the ITU-R P.839-4 recommended constant annual means of 4.74, 4.79, 4.84, and 4.87 km for the Sahel, Midland, Guinea Savanna, and Coastal Zones, respectively. Inaccurate estimation of rain height can lead to either underestimation or overestimation of rain-induced attenuation.

Similarly, ITU-R P.839-4 prescribes a constant rain height of about 4.54 km for Pretoria, whereas a recent study revealed that rain height varies seasonally with maximum and minimum values of about 5,520 m and 4,357 m in the summer and winter, respectively [15]. Incorporating seasonal rain height characterization enhances the reliability of propagation models such as the ITU-R P.618 on rain attenuation and system performance. Analyses have indicated that integrating localized rain height data improves model accuracy thus enhances the reliability of the communication system designs [16]. The aim of this study is to utilize the novel seasonal rain height data provided by the recent study in [15] to compute seasonal rain-induced attenuations at Super High Frequency (SHF) and Extra High Frequency (EHF).

II. RESEARCH LOCATION AND METHODOLOGY

A. Radio propagation parameters for the earth-space link

The space station used for the study is the Intelsat 20 (IS-20) satellite positioned at 68.5° in a Geostationary Earth Orbit (GEO). It has a partial footprint in Africa, Asia, Europe, and the Middle East, providing digital cable TV and communication services, such as broadband internet services. Although the satellite operates at C and Ku bands, the present study investigates the potential effects of rain-induced attenuation at Ka and V bands for future upgrades. These are higher frequency bands required to fulfill the continuous demand for uninterrupted high-speed internet services [1]. The earth station for the study is the Soshanguve Campus of Tshwane University of Technology, Pretoria, South Africa. The coordinates of the station are -25.541° S, 28.097° E, and the elevation is 1344 m above mean sea level [17]. Soshanguve is a town in the northern part of Pretoria. Pretoria is generally categorized as a humid subtropical climate according to the Köppen climate classification. It experiences cool, dry winters (June-August), hot, rainy summers (December-February), and transition seasons referred to as autumn (March-May) and spring (September-November) [18]-[20]. The IS-20 satellite can be tracked and maintained at optimal performance in Pretoria through a line of sight at an elevation angle of 31.5° from the horizon [21]. The satellite and ground station parameters used for calculating the rain-induced attenuations are presented in Table 1.

TABLE 1. THE EARTH STATION AND SATELLITE PARAMETERS USED FOR COMPUTATION OF RAIN-INDUCED ATTENUATION

Parameters	Input values
Ground Station Latitude	25.542°S
Antenna Elevation	31.5°
Antenna Height above sea level (m)	1,346 m
1min Rain Rate at 0.01% exceedance	84.5 mm/hr
Autumn Rain Height (m)	4,732 m
Winter Rain Height (m)	4,308 m
Spring Rain Height (m)	4,853 m
Summer Rain Height (m)	5,217 m
Satellite Name	IS-20
Satellite position	68.5° E (GEO)

B. Computation of rain-induced attenuation

The measured seasonal rain heights at Pretoria reported recently by Lawal *et al.* [15] and the rain rate of 84.5 mm/hr at 0.01% exceedance reported by Ojo [22] are presented in Table 1. The selected frequency bands that lie within the SHF and EHF are the Ka and V bands. The proposed uplink and downlink frequencies used for the study are presented in Table 2. The ITU-R procedure was adopted for calculating rain-induced attenuation. This model uses rain parameters (rain rate, rain height), ground station parameters (ZDH, elevation angle, latitudinal coordinate), and the radio wave parameters (frequency, polarization) to determine the long-term rain attenuation statistics for point rainfall for frequencies up to 55 GHz [23].

TABLE 2. TRANSMISSION FREQUENCIES USED FOR COMPUTATION OF RAIN-INDUCED ATTENUATION

Link Frequency	Ka	V
Downlink Frequency (GHz)	20	40
Uplink Frequency (GHz)	30	50

This procedure remains the most widely accepted model and has been proved to be efficient in different parts of the world, such as Oyo, Nigeria [24], North America [25], seven stations in India [26], thirty-five stations in Venezuela [27], forty-two stations in Columbia [28], five stations in Libya [29], and Durban [30]. The details of the procedure for the computation of long-term rain attenuation are as follows.

Step 1: Determine the slant-path L_s *(km)* between the satellite and the earth station antenna at height h_s above the mean sea level with elevation angle θ using equation (1)

$$for\ \theta \geq 5^o \quad L_S = \frac{h_r - h_S}{\sin\theta} \ \text{(km)} \tag{1}$$

$$for\ \theta < 5^o \qquad L_s = \frac{2(h_r - h_s)}{[sin^2\,\theta + 2(h_r - h_s)/R_e]^{\frac{1}{2}} + sin\,\theta} \ \text{(km)} \tag{2}$$

where h_r is the rain height in km, h_s is height of the ground station above sea level and R_e is the effective Earth radius assumed to be 8,500 km

Step 2: Calculate the horizontal projection L_H of the slant path length using equation (3).

$$L_H = L_s\,cos\,\theta \qquad \text{(km)} \tag{3}$$

Step 3: Compute the specific attenuation using the power-law relationship below.

$$\gamma_{0.01} = aR_{0.01}^b \quad \text{(dB/km)} \tag{4}$$

where *a* and *b* are parameters which depend on frequency and be obtained from ITU-R P.530-18 recommendation [31].

Step 4: The horizontal component of the reduction factor for 0.01% of time is given by equations (5).

$$r_{0.01} = \frac{1}{1 + 0.78\sqrt{\frac{L_H\gamma_{0.01}}{f}} 0.381(1 - e^{-2L_H})} \tag{5}$$

Step 5: The vertical adjustment factor $v_{0.01}$ for 0.01% of time is given by equations (9) subject to the conditions in equations (6)-(8).

$$\text{Let} \quad \xi = tan^{-1}\left[\frac{h_r - h_s}{L_H r_{0.01}}\right]^o \tag{6}$$

$$\text{For } \xi > \theta \qquad L_R = \frac{L_H r_{0.01}}{cos\,\theta} \qquad \text{(km)} \tag{7}$$

$$\text{Else} \qquad L_R = \frac{(h_r - h_s)}{sin\,\theta} \qquad \text{(km)} \tag{8}$$

If $|\phi| < 36^o; \quad \chi = 36 - |\phi|$

Else $\chi = 0^o$

$$v_{0.01} = \frac{1}{1 + \sqrt{sin\,\theta}\left(31(1 - e^{-[\frac{1}{(1+\chi)}])}\left[\sqrt{\gamma_{0.01}L_R}/f^2 - 0.45\right]\right)} \tag{9}$$

where ϕ represents the earth station's latitude.

Step 6: Calculate the effective path length L_E using equation (10)

$$L_E = L_R v_{0.01} \qquad \text{(km)} \tag{10}$$

Step 7: The average annual rain-induced attenuation $A_{0.01}$ for 0.01% of time is calculated as;

$$A_{0.01} = \gamma_{0.01}L_E \quad \text{(dB)} \tag{11}$$

Step 8: The long-term rain-induced attenuation A_p exceeded for any time percent p for average year is determined using equation (12) subject to the conditions below.

If $p \geq 1\% \quad or \quad |\phi| \geq 36^o \quad then\ \beta = 0$

If $p < 1\%, \quad |\phi| < 36^o and\ \ \theta \geq 25^o\ \ then$

$$\beta = -0.005(|\phi| - 36)$$

Otherwise $\beta = -0.005(|\phi| - 36) + 1.8 - 4.25\,sin\,\theta$

$$A_p = A_{0.01}\left[\frac{p}{0.01}\right]^{-[0.655 + 0.033\,ln(A_{0.01}) - \beta(1-p)\,sin\,\theta]} \text{(dB)} \tag{10}$$

III. RESULTS AND DISCUSSIONS

A. Implications of Seasonal Rain Heights on Rain-induced Attenuation

The four seasonal rain heights and other input parameter were applied to compute the rain-induced attenuation at the selected frequencies by following the procedure above. Figs. 1-4 present the attenuation obtained for different percentages of time exceeded in a year for the selected uplink and downlink frequencies in Ka and V Bands shown in Table 1.

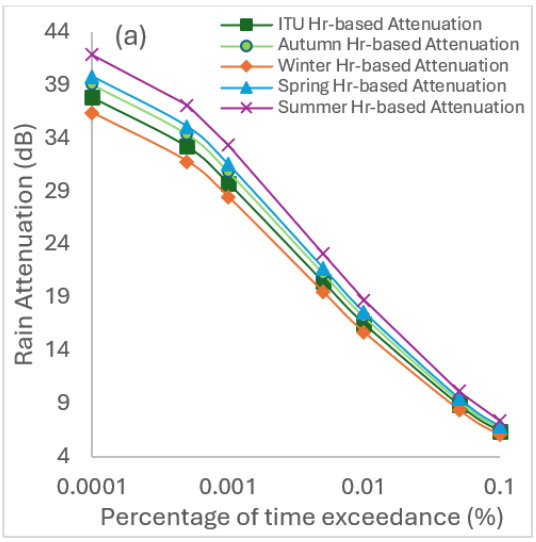

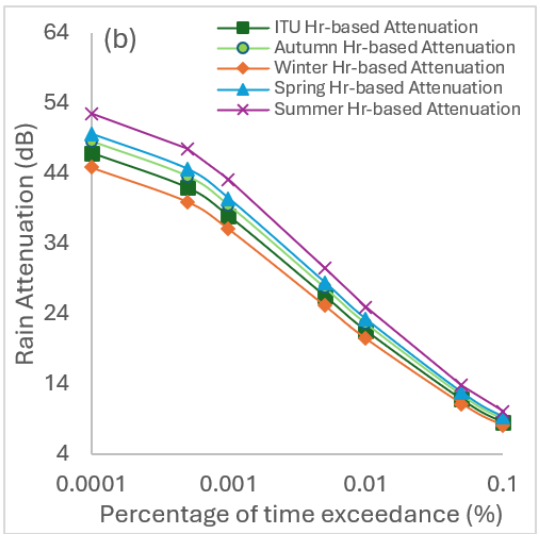

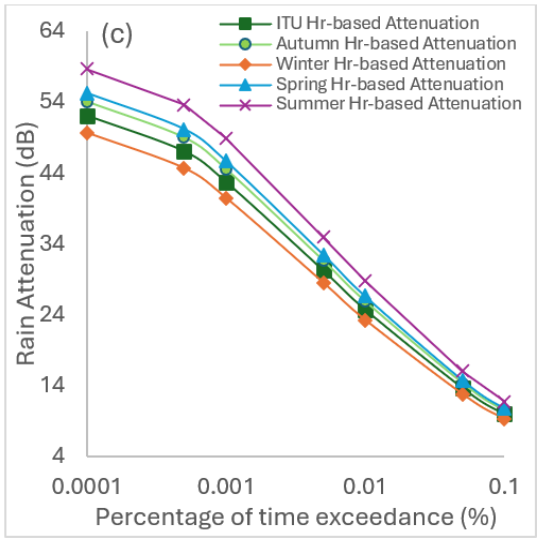

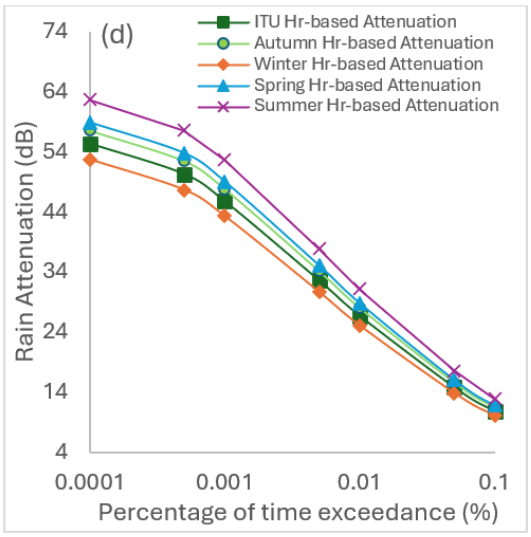

Fig. 1. Estimated Rain-induced attenuations at (a) Ka Band Uplink Frequency 20 GHz, (b) Ka Band Downlink Frequency 30 GHz, (c) V Band Uplink Frequency 40 GHz, and (d) V Band Uplink Frequency 50 GHz

The results of the computations indicate significant differences in attenuation for various rain heights while other input parameters are fixed. The attenuations at all the frequencies follow the same trend. Generally, the attenuation increases proportionately with frequency but varies seasonally, hence the reason to determine the magnitudes of attenuation at high frequencies [32]-[33]. The attenuation rises as the percentage of time exceedance for a specific value is lowered at all the frequencies considered. This implies a that higher fade margin must be provided to reduce the percentage of time at which attenuation exceeds certain thresholds. Least attenuations were observed during the winter season due to the minimum value of rain height shown in Table 1. The extremely cool and dry weather during the winter in Pretoria as reported by Koppen [18] and South African Weather Service [34] is responsible for the low rain height which resulted in the least attenuation compared to other seasons. The melting rate of the bright band (melting layer) is grossly reduced because low solar radiation reaches the earth portion (Pretoria) in the winter season. The rain height increases gradually as the weather transitions from the extremely cool winter to the hot, wet summer via the autumn season. The increase in rain height from 4,308 m in winter to about 4,732 m in the autumn resulted in a consequential increase in rain attenuation as depicted in Figures 1 and 2. The summer is the hottest season, which causes a high melting rate of the bright band, thereby raising the rain height. Consequently, maximum attenuation is experienced at all frequencies in the summer, followed by a gradual decline as the spring approaches.

It could be observed from Figure 2 that the differences between the seasonal-based Hr attenuation and the fixed ITU Hr-based attenuation vary significantly, which is the aim of this research. For instance, at a 0.1% exceedance in the Ka Band Downlink frequency of 20 GHz, attenuation during the winter is 6.04 dB while it is 7.35 dB in the summer, leading to a percentage difference of 21.7%. For the same frequency at 0.0001%

exceedance, the winter attenuation is 36.4 dB whereas it is up to 41.9 dB in the summer indicating a percentage difference of 15.1%. Similarly, the winter and summer attenuations have the widest margins at all frequencies with a maximum percentage difference of about 26% occurring at 0.1% exceedance for 50 GHz V band uplink. Table 3 presents the expected attenuation that must be offset to achieve certain percentage of signal availability in a year. It should be noted that the fade margin required to achieve an efficient radio communication link during rainfall must be greater than or equal to the estimated attenuations in Table 3. Hence, an appropriate fade mitigation technique (FMT) must be employed so that the resulting fade margins satisfy equation (13) below [35].

$$Fmargin \geq Ap \quad \text{(dB)} \tag{13}$$

where Ap is the attenuation at $p\%$ of exceedance.

TABLE 3. COMPUTED SEASONAL RAIN-INDUCED ATTENUATIONS BASED ON RAIN HEIGHT VARIABILITY FOR EARTH-SPACE LINKS IN PRETORIA

Operating Frequency	% of signal availability per year	Summer Attenuation (dB)	Autumn Attenuation (dB)	Winter Attenuation (dB)	Spring Attenuation (dB)
20 GHz (Ka D/L)	99.9	7.35	6.67	6.04	6.85
	99.99	18.76	17.19	15.71	17.59
	99.999	33.4	30.88	28.49	31.53
30 GHz (Ka U/L)	99.9	10.07	9.04	8.09	9.30
	99.99	24.96	22.63	20.46	23.22
	99.999	43.16	39.52	36.10	40.45
40 GHz (V D/L)	99.9	11.76	10.48	9.32	10.81
	99.99	28.72	25.88	23.26	26.60
	99.999	48.93	44.57	40.50	45.68
50 GHz (V U/L)	99.9	12.89	11.44	10.13	11.81
	99.99	31.20	28.01	25.09	28.83
	99.999	52.73	47.86	43.35	49.10

B. Comparison of Seasonal Hr-based with ITU Hr-based Attenuations

The seasonal Hr-based attenuations were compared with the ITU Hr-based attenuation to study the influence of rain height variability on the estimated attenuations during the four seasons. Figures 1 and 2 revealed that the ITU Hr underestimated attenuations in the summer, autumn, and spring while the winter season values were overestimated. Figure 2 specifically provides a detailed comparison of the 20 GHz attenuations at 0.01% of time exceedance. It could be observed that ITU Hr recommended a fixed attenuation of 16.53 dB, whereas the seasonal rain heights revealed varying attenuations of 17.9 dB, 15.59 dB, 17.59 dB, and 18.76 dB in the autumn, winter, spring, and summer, respectively.

At 0.01% exceedance, which is the most widely recommended exceedance level, the estimated worst season rain-induced attenuations are 18.76, 24.96, 28.72, and 31.20 dB for 20 GHz, 30 GHz, 40 GHz, and 50 GHz respectively. This implies that 99.99% signal availability could be achieved annually on earth-space links operating at these frequencies in Pretoria, if the link budget is properly designed to accommodate fade margins greater than the estimated attenuations. The findings of this research show that the differences between estimated attenuation based on measured seasonal rain height and the recommended ITU-R fixed rain height could be as high as 8 dB and 10 dB at Ka and V bands, respectively.

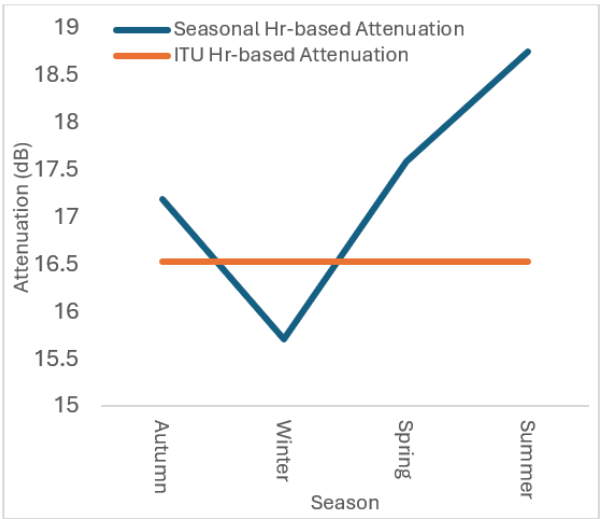

Fig.2. Seasonal variation of rain-induced attenuation at 20 GHz for 0.01% exceedance

IV. CONCLUSIONS

This research confirms the consequence of rain height variation on rain-induced as established by previous studies conducted in other regions of the world. It also recommended seasonal attenuations for radio links operating at frequencies in the Ka and V bands in Pretoria. The research recommended varying fade margins required to achieve a certain percentage of signal availability over the seasons, unlike the ITU HR-based attenuation, which recommended a fixed value throughout the seasons annually. This would assist local radio engineers to dynamically determine the appropriate minimum fade margins that would accommodate the recommended attenuations at different seasons. Consequently, the quality of received signal strength in all seasons can be improved. Although the research has revealed seasonal variation of attenuation due to rain height variability, it is recommended that a local radio spectrum observatory laboratory be set up in the study location so that experimentally measured rain-induced attenuation could be compared with the estimated seasonal values reported in this work.

ACKNOWLEDGEMENT

The authors received funding from the Tshwane University of Technology, South Africa.

REFERENCES

[1] A. Goldsmith, *Wireless Communications*. Cambridge University Press, 2005.

[2] A. J. Paulraj, R. Nabar, and D. Gore, *Introduction to Space-Time Wireless Communications*. Cambridge University Press, 2003.

[3] J. G. Andrews, S. Buzzi, W. Choi, S. V. Hanly, A. Lozano, and A. C. K. Soong, "What will 5G be?," *IEEE Journal on Selected Areas in Communications*, vol. 32, no. 6, pp. 1065–1082, June 2014.

[4] R. W. Heath, *Foundations of MIMO Communication*. Cambridge University Press, 2018.

[5] C. Han, L. Feng, J. Huo, Z. Deng, G. Zhang, B. Ji, Y. Zhou, Y. Bi, S. Duan, and R. Yuan, "Characteristics of rain-induced attenuation over signal links at frequency ranges of 25 and 38 GHz observed in Beijing," *Remote Sensing*, vol. 13, no. 11, p. 2156, 2021. [Online]. Available: https://doi.org/10.3390/rs13112156

[6] A. Adekola, B. Smith, and C. Johnson, "Improving rain attenuation prediction using the Quasi-Moment-Method (QMM)," *Journal of Atmospheric and Telecommunication Sciences*, vol. 45, no. 2, pp. 123–135, 2023. [Online]. Available: https://doi.org/10.14209/jcis.2023.22

[7] J. S. Ojo and P. A. Owolawi, "Characterization of rain heights due to 0° isotherm in tropical and subtropical climates: Implication on rain-induced attenuation prediction," *Theoretical and Applied Climatology*, vol. 135, pp. 331–340, 2019. [Online]. Available: https://doi.org/10.1007/s00704-018-2382-z

[8] International Telecommunication Union, "Characteristics of precipitation for propagation modelling (Recommendation ITU-R P.837-7)," Geneva, Switzerland, 2017. [Online]. Available: https://www.itu.int/rec/R-REC-P.837-7-201706-I/en

[9] International Telecommunication Union, "Rain height model for prediction methods (Recommendation ITU-R P.839-4)," Geneva, Switzerland, 2013. [Online]. Available: https://www.itu.int/rec/R-REC-P.839-4-201303-I/en

[10] L. Lin, S. Zhang, X. Zhang, X. Hao, Z. Zhao, Q. Zhu, and R. Zhang, "Weighted mean annual rain height applied to rain attenuation prediction on earth-space links," *International Journal of Antennas and Propagation*, Article ID 4162415, 2022. [Online]. Available: https://doi.org/10.1155/2022/4162415

[11] J. S. Mandeep, "Rain height statistics for satellite communication in Malaysia," *Journal of Atmospheric and Solar-Terrestrial Physics*, vol. 70, pp. 1617–1620, 2008.

[12] F. A. Semire, R. Mohd-Mokhtar, and Z. K. Adeyemo, "Statistical analysis of rain height over Malaysia," *Radioelectronics and Communications Systems*, vol. 59, no. 9, pp. 423–426, 2016. [Online]. Available: https://doi.org/10.3103/S0735272716090065

[13] Y. B. Lawal, S. E. Falodun, and J. S. Ojo, "Temporal evolution of atmospheric parameter-profiling on rain height over two geoclimatic regions in Nigeria," *Journal of Atmospheric and Solar-Terrestrial Physics*, vol. 211, p. 105482, 2020. [Online]. Available: https://doi.org/10.1016/j.jastp.2020.105482

[14] Y. B. Lawal, S. E. Falodun, J. S. Ojo, and E. O. Olurotimi, "Geoclimatic characterization and latitudinal dependence of rain heights over Nigeria," *Journal of Physics: Conference Series*, vol. 2034, no. 1, p. 012010, 2021.

[15] Y. B. Lawal, P. A. Owolawi, C. Tu, E. Van Wyk, and J. S. Ojo, "The kernel density estimation technique for spatio-temporal distribution and mapping of rain heights over South Africa: The effects on rain-induced attenuation," *Atmosphere*, vol. 15, no. 11, p. 1354, 2024. [Online]. Available: https://doi.org/10.3390/atmos15111354

[16] J. S. Mandeep and J. E. Allnutt, "Rain attenuation predictions at Ku-band in South East Asia countries," *Progress In Electromagnetics Research*, vol. 76, pp. 65–74, 2007. [Online]. Available: https://doi.org/10.2528/PIER07062605

[17] "Flood risk map and analysis." [Online]. Available: https://www.floodmap.net/?gi=954013

[18] W. Köppen and R. Geiger, "Das geographische System der Klimate (The geographical system of climates)," in *Handbuch der Klimatologie*, W. Köppen and R. Geiger, Eds., vol. 1, part C, Gebrüder Borntraeger, 1936.

[19] M. Kottek, J. Grieser, C. Beck, B. Rudolf, and F. Rubel, "World map of the Köppen-Geiger climate classification updated," *Meteorologische Zeitschrift*, vol. 15, no. 3, pp. 259–263, 2006. [Online]. Available: https://doi.org/10.1127/0941-2948/2006/0130

[20] A. C. Kruger and M. P. Nxumalo, "Historical rainfall trends in South Africa: 1921–2015," *Water SA*, vol. 43, no. 2, pp. 285–297, 2017. [Online]. Available: https://doi.org/10.4314/wsa.v43i2.12

[21] T. Soler and H. M. Eisemann, "Determination of look angles to geostationary communication satellites," *Journal of Surveying Engineering*, vol. 120, no. 2, pp. 94–107, 1994. [Online]. Available: http://dx.doi.org/10.1061/(ASCE)0733-9453(1994)120:3(115)

[22] J. S. Ojo and P. A. Owolawi, "Development of one-minute rain-rate and rain-attenuation contour maps for satellite propagation system planning in a subtropical country: South Africa," *Advances in Space Research*, vol. 54, no. 8, pp. 1487–1501, 2014. [Online]. Available: https://doi.org/10.1016/j.asr.2014.06.028

[23] ITU-R P.618-13, "Propagation data and prediction methods required for the design of Earth-space telecommunication systems," International Telecommunication Union, Radiocommunication Section (ITU-R), Geneva, Switzerland, 2017.

[24] H. O. Busari and O. A. Fakolujo, "Estimation of attenuation due to rain within Ka and Ku bands in Oyo State, Nigeria," *FUOYE Journal of Engineering and Technology (FUOYEJET)*, vol. 6, no. 1, 2021.

[25] K. Chakravarty and A. Maitra, "Rain attenuation studies over an earth–space path at a tropical location," *Journal of Atmospheric and Solar-Terrestrial Physics*, vol. 72, no. 1, pp. 135–138, 2010.

[26] P. Panchal and R. Joshi, "Performance analysis and simulation of rain attenuation models at 12–40 GHz band for an earth-space path over Indian cities," *Procedia Computer Science*, vol. 79, pp. 801–808, 2016. [Online]. Available: https://doi.org/10.1016/j.procs.2016.03.110

[27] A. D. Pinto Mangones, L. Garcia, A. Diaz, and J. Lozano, "Rainfall rate and rain attenuation contour maps for preliminary 'Simon Bolivar' satellite links planning in Venezuela," *DYNA*, vol. 86, no. 211, pp. 47–57, 2019.

[28] L. D. Emiliani, A. Pantoja, A. Jimenez, and J. Castellanos, "Development of rain attenuation and rain-rate maps for satellite system design in the Ku and Ka bands in Colombia," *IEEE Antennas and Propagation Magazine*,

vol. 46, no. 6, pp. 54–68, Dec. 2004. [Online]. Available: https://doi.org/10.1109/MAP.2004.1396736

[29] M. R. Islam, M. M. Rahman, and S. Hasan, "Performance analysis of rain attenuation on earth-to-satellite microwave links design in Libya," in *Proceedings of the 6th International Conference on Mechatronics (ICOM)*, Kuala Lumpur, Malaysia, 2017, pp. 1–6.

[30] E. O. Olurotimi, S. E. Falodun, and J. S. Ojo, "Analysis of bright-band height data from TRMM-PR for satellite communication in Durban, South Africa," in *Proceedings of AFRICON 2015*, Addis Ababa, Ethiopia, Sep. 2015, pp. 1–5. [Online]. Available: https://doi.org/10.1109/AFRCON.2015.7331927

[31] ITU-R P.530-18, "Propagation data and prediction methods required for the design of terrestrial line-of-sight systems," International Telecommunication Union, Geneva, Switzerland, 2021. [Online]. Available: https://www.itu.int/rec/R-REC-P.530-18-202109-I/en

[32] O. M. Alade, "Standardization of attenuation formula for radio waves propagation through free space (LOS) communication links," *Science Journal of Physics*, Article ID sjp-281, pp. 1–7, 2012. [Online]. Available: https://doi.org/10.7237/sjp/281

[33] Y. B. Lawal, S. E. Falodun, J. S. Ojo, and S. O. Oyelami, "Rain height statistics from GPM data for satellite communications systems in Nigeria," *IOP Conference Series: Earth and Environmental Science*, vol. 655, p. 012038, 2021. [Online]. Available: https://doi.org/10.1088/1755-1315/655/1/012038

[34] South African Weather Service, "South African climate," 2021. [Online]. Available: https://weathersa.co.za

[35] K. Vaclav and G. Martin, "Rain attenuation at 58 GHz: Prediction versus long-term trial results," *EURASIP Journal on Wireless Communications and Networking*, vol. 2007, no. 1, pp. 46–46, 2007. [Online]. Available: https://doi.org/10.1155/2007/297931